



# Effect of changes in continuous carboxylate feeding on the specific production rate of butanol using *Clostridium saccharoperbutylacetonicum*

Florian Gattermayr<sup>a,b,\*</sup>, Christoph Herwig<sup>b,c</sup>, Viktoria Leitner<sup>a</sup>

<sup>a</sup> Division Wood Chemistry and Biotechnology, Kompetenzzentrum Holz GmbH, Altenberger Strasse 69, 4040 Linz, Austria

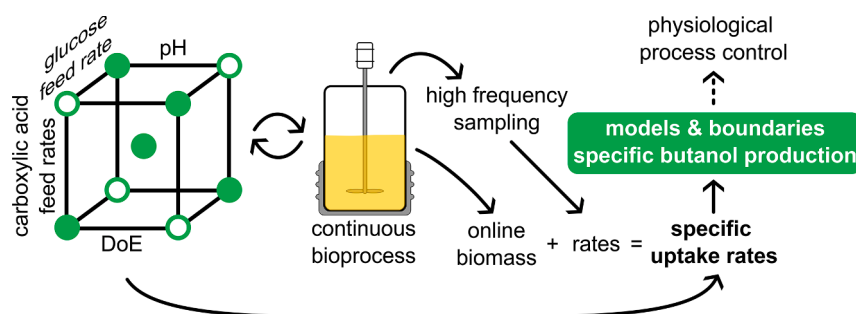
<sup>b</sup> Institute of Chemical Engineering, Vienna University of Technology, Getreidemarkt 9/166, 1060 Vienna, Austria

<sup>c</sup> Competence Center CHASE GmbH, Altenberger Strasse 69, 4040 Linz, Austria

## HIGHLIGHTS

- Uptake rates of carboxylic acids were modeled during continuous butanol fermentation.
- Organic acid feed rate and their ratio significantly influence their uptake.
- High uptake rates of glucose and butyric acid increase production rate of butanol.
- Ideal conditions for a stable continuous butanol fermentation process are proposed.

## GRAPHICAL ABSTRACT



## ARTICLE INFO

### Keywords:

Butanol fermentation  
*Clostridium saccharoperbutylacetonicum*  
 Continuous culture  
 Design of experiments  
 Multi-feedstock biorefinery

## ABSTRACT

Substrate variability in multi-feedstock biorefineries has implications for the stability of downstream bio-processes. Here, we studied potential effects of fluctuating feed rates and pH on substrate uptake and butanol production by *Clostridium saccharoperbutylacetonicum* during continuous co-feeding with butyric and acetic acid. Monitoring the fermentation extensively and at high frequency, enabled us to perform irregular fraction experimental designs. The total acid feed rate and the ratio of butyric acid to acetic acid in the feed were found to be significant factors in their uptake by the culture. Furthermore, to maximize the specific butanol production rate, glucose may not be limited and butyric acid should be supplied at a rate of  $7.5 \text{ mmol L}^{-1} \text{ h}^{-1}$ . Surprisingly, pH played a role only indirectly, in its effect on process stability. Obtained results facilitate the control of feed rates based on physiological descriptors, which will be a critical factor in the establishment of multi-feedstock biorefineries.

## 1. Introduction

Under the growing negative impacts of man-made climate crisis on agricultural production, the efficient and holistic use of waste streams

for the provision of high value-added chemicals is more important than ever. In this context, advanced multi-feedstock biorefineries, were miscellaneous and inhomogeneous substrates, such as food wastes and lignocellulosic residuals, can be utilized, are considered a promising

\* Corresponding author at: Division Wood Chemistry and Biotechnology, Kompetenzzentrum Holz GmbH, Altenberger Strasse 69, 4040 Linz, Austria.

E-mail address: [f.gattermayr@wood-kplus.at](mailto:f.gattermayr@wood-kplus.at) (F. Gattermayr).

approach. However, processing these feedstocks is a challenging task due to their volatile composition and quality as well as their seasonal variability. A possible solution to cope with these issues is the use of anaerobic undefined mixed cultures for the production of carboxylates which can act as intermediates for further conversion steps leading to a great variety of bioproducts (Agler et al., 2011). This is generally referred to as the *carboxylate platform* as compared to other common biorefinery platforms like the sugar or syngas platform (Holtzapfel and Granda, 2009; Cherubini et al., 2009). Obtained carboxylic acids specifically butyric acid and acetic acid can then be used as co-substrates for the fermentation of solvents, which leads to an increased productivity thereof compared to solely using glucose as carbon source (Chen and Blaschek, 1999; Tashiro et al., 2004; Tashiro et al., 2007; Baba et al., 2012). Unfortunately, monomeric sugars are still needed, since they serve both as a source of ATP and electrons for the conversion of butyric acid to butanol and as carbon source for microbial growth (Richter et al., 2012). The fundamental reason for carboxylic acid uptake to be possible in the first place, lies in the physiology of acetone-butanol-ethanol (ABE) producing clostridia, which consists of two characteristic phases: the acidogenic (exponential phase) and the solventogenic phase (mainly stationary phase and therefore non-growth-associated). Acids formed in the first phase function, due to their pH lowering effect and their increasing concentrations, as inductor for the following solventogenic phase in which they are re-assimilated and converted to solvents (Jones and Woods, 1986; Bahl et al., 1982; Grupe and Gottschalk, 1992; Matta-El-Ammouri et al., 1987). This can be considered as a detoxification reaction to deal with increasing levels of undissociated acids which in this form can easily pass the membrane of cells and so cause detrimental effects (Herrero, 1983; Fond et al., 1985; Maddox et al., 2000; Hüse-mann and Papoutsakis, 1988).

On this basis and considering that the concentrations and composition of the produced carboxylates are still affected by a high variability and volatility of the initial substrate (Arslan, 2014), it is only now that one thing becomes fully apparent: For an efficient and continuous production of solvents it is necessary to have profound knowledge of how feed rates of carboxylic acids and sugars together with the pH impact fermentation. Hence, our hypothesis: understanding the behavior and dynamics of specific substrate uptake rates in dependence of fermentation parameters such as feed rates and pH is crucial for the development of practicable models. This also includes defining the optimal process conditions for the specific biological production system. Our goal was to gather scalable process understanding for continuous ABE fermentations. This was achieved by a Design of Experiments (DoE) approach to study substrate uptake depending on the four factors pH, the ratio of acetic and butyric acid in the feed, the total organic acid feed rate, and the glucose feed rate in proportion to the total organic acid feed rate. Ultimately, also the specific butanol production rate could be described by two physiological descriptors: the specific uptake rate of both butyric acid and glucose. While there are many studies which focus on partial aspects like operating continuous cultures (Zheng et al., 2013; Elbesh-bishy et al., 2015; Mutschlechner et al., 2000) or co-feeding of carboxylic acids (Richter et al., 2012; Tashiro et al., 2004; Oshiro et al., 2010) we present here a novel approach by bringing together an advanced high-frequency monitoring strategy and a sophisticated reactor setup to enable the implementation of DoE within a continuous single stage fermentation.

## 2. Material and methods

### 2.1. Organism and culture conditions

*Clostridium saccharoperbutylacetonicum* N1-4 (HMT) type strain 14923 (DSMZ, Germany) was used for all fermentation experiments in this study. The cells were stored at  $-80\text{ }^{\circ}\text{C}$  in the form of spores in a modified mineral medium (Monot et al., 1982; Standfest, 2013) aliquoted in cryogenic tubes to 180  $\mu\text{L}$  each. A preculture was prepared by

aseptically transferring the content of one such tube into 10  $\mu\text{L}$  of anaerobic clostridial growth medium (CGM, see Section 2.2) with a glucose concentration of  $10\text{ g L}^{-1}$ , heat-shocked in boiling water for 1 min, cooled down and incubated standing at  $30\text{ }^{\circ}\text{C}$  for 24 h. 6  $\mu\text{L}$  of this preculture were then transferred to 54  $\mu\text{L}$  of CGM (final glucose concentration was  $20\text{ g L}^{-1}$ ) and left standing at  $30\text{ }^{\circ}\text{C}$  for another 12 h. Eventually, this culture was used to inoculate the reactor via overpressure of sterile nitrogen gas.

### 2.2. Media

If not stated otherwise, all chemicals were obtained from Carl Roth, Germany. For the continuous fermentation experiments, a CGM (Wiesenborn et al., 1988) was modified to reduce the amount of yeast extract and phosphate. Dissolved in deionized water it contained  $2.5\text{ g L}^{-1}$  yeast extract,  $2\text{ g L}^{-1}$   $(\text{NH}_4)_2\text{SO}_4$  (Acros Organics, USA),  $0.712\text{ g L}^{-1}$   $\text{MgSO}_4 \cdot 7\text{H}_2\text{O}$  (Sigma Aldrich, USA),  $0.015\text{ g L}^{-1}$   $\text{FeSO}_4 \cdot 7\text{H}_2\text{O}$ ,  $0.015\text{ g L}^{-1}$   $\text{KH}_2\text{PO}_4$ ,  $0.015\text{ g L}^{-1}$   $\text{K}_2\text{HPO}_4$ ,  $0.01\text{ g L}^{-1}$   $\text{NaCl}$ ,  $1.5\text{ g L}^{-1}$  L-(+)-asparagine monohydrate,  $0.01\text{ g L}^{-1}$   $\text{MnSO}_4 \cdot \text{H}_2\text{O}$ , and  $0.139\text{ g L}^{-1}$   $\text{K}_2\text{SO}_4$  (Sigma Aldrich, USA) to compensate for the missing potassium caused by the reduction of phosphate salts. It was autoclaved for 15 min at  $121\text{ }^{\circ}\text{C}$ . Any glucose (anhydrous D-(+)-glucose) solution was prepared and autoclaved separately under the same conditions to prevent a Maillard reaction. Subsequently, the evaporated water was replaced with sterile deionized water under aseptic conditions while simultaneously adding  $0.9\text{ g L}^{-1}$  L-(+)-cysteine hydrochloride through a sterile syringe filter (0.2  $\mu\text{m}$ , VWR, Germany). Still hot, the medium was either purged (in the case of the fermentation vessel) or the headroom was replaced with sterile nitrogen gas to hinder oxygen from dissolving into the liquid. The CGM for both pre-cultures differed slightly and contained  $5\text{ g L}^{-1}$  yeast extract,  $0.075\text{ g L}^{-1}$   $\text{KH}_2\text{PO}_4$ ,  $0.075\text{ g L}^{-1}$   $\text{K}_2\text{HPO}_4$  and no  $\text{K}_2\text{SO}_4$ , while all other ingredients were kept the same as specified above. To set any feed rate related factors as described in Section 2.5, four different feeds were prepared: (i) glucose feed (CGM containing  $200\text{ g L}^{-1}$  glucose) (ii) CGM feed (CGM only) (iii) acetic acid feed (CGM containing  $25\text{ g L}^{-1}$  acetic acid) (iv) butyric acid feed (CGM containing  $18\text{ g L}^{-1}$  butyric acid).

### 2.3. Bioreactor fermentations

For the continuous fermentations, a DASGIP® bioreactor system (Eppendorf, Germany) was used. It was controlled at  $30\text{ }^{\circ}\text{C}$ , stirred at 100 rpm and constantly purged via a mass flow controller (Bronkhorst, Netherlands) with  $5\text{ sL h}^{-1}$  of sterile  $\text{N}_2$  5.0. The custom made glass vessel with a working volume ( $V_r$ ) of 0.6 L had a screwed fitting on its side to accommodate the optical density probe (Optek ASD12-N-10-L225, Germany). A pH probe and a redox probe (both Mettler Toledo, Switzerland/USA) were used to measure pH and redox potential, respectively. With an initial glucose concentration of  $20\text{ g L}^{-1}$  and a starting pH of 7.1, fermentations were initially performed as batch for 12 h. The pH was unregulated during this process until it reached 5.6. Then, the pH control was activated, which regulated the pH by dosing  $5\text{ mol L}^{-1}$   $\text{NaOH}$  and  $5\text{ mol L}^{-1}$   $\text{HCl}$ . After the batch phase was over the setpoint of the pH controller was adjusted according to the experimental plan and the feeding pumps and the effluent pump were started to ensure an overall dilution rate ( $D$ ) of  $0.075\text{ h}^{-1}$ . Each individual feed rate was set in a separate reactor script which controlled the corresponding peristaltic feed pump. By logging the scale values of each feed, we were able to calculate the effective feed rates in real time, compare them to the setpoints and adjust the calibration factors of the pumps accordingly if necessary. A few drops of a 10 % (v/v) Antifoam 204 (Sigma Aldrich, USA) solution were added automatically every 3 h to keep foam levels low. Offgas was cooled down by a heat exchanger using an external thermostat (Julabo FP 40, Germany) set to  $13\text{ }^{\circ}\text{C}$  to re-condensate water and solvent vapor as well as to protect the instruments downstream. Samples were taken frequently and automatically with a Cavro XCalibur Pump (Tecan, Switzerland), dispensed in

deep-well plates with a custom built robot to be later analyzed by HPLC (see Section 2.4). To conserve the state of the sample at sampling time, the cells were fixated by adding glutaraldehyde (Alfa Aesar, USA) for a final concentration of 0.5 % (v/v).  $\text{H}_2\text{SO}_4$  was added as well to match the concentration of  $5 \text{ mmol L}^{-1}$  in the eluent for HPLC analysis. A schematic of the whole fermentation setup is depicted in Fig. 1.

#### 2.4. Analytics

The determination of glucose, carboxylates, and alcohols was done by analyzing sterile filtrated ( $0.2 \mu\text{m}$ , PALL, USA) samples with an HPLC system (Shimadzu Prominence, Japan). It consisted of an Aminex HPX-87H ( $300 \times 7.8 \text{ mm}$ ) column (Biorad, USA) operated at a temperature of  $40 \text{ }^\circ\text{C}$  using  $5 \text{ mmol L}^{-1} \text{ H}_2\text{SO}_4$  as eluent at a flow rate of  $0.6 \text{ mL min}^{-1}$ . Detection was achieved by RID and DAD at a wavelength of  $210 \text{ nm}$  and  $269 \text{ nm}$ . Offgas ( $\text{N}_2$ ,  $\text{H}_2$ ,  $\text{CO}_2$ ,  $\text{O}_2$ ) was analyzed with a micro GC (Inficon, Switzerland) equipped with a thermal conductivity detector. Separation occurred in two columns, an RT-Molsieve 5A  $0.25 \text{ mm}$  ( $10 \text{ m}$ ) operated at  $30 \text{ psi}$  and a constant temperature of  $80 \text{ }^\circ\text{C}$  as well as an RT-Q-BOND ( $12 \text{ m}$ ) operated at  $30 \text{ psi}$  with a programmed temperature gradient ( $20 \text{ s}$

at  $80 \text{ }^\circ\text{C}$  after ramping it up at a rate of  $1.5 \text{ }^\circ\text{C s}^{-1}$  to  $240 \text{ }^\circ\text{C}$  and holding it there for  $40 \text{ s}$ ). The carrier gas was argon. For real time cell dry weight (CDW) determination, measurement data collected from the optical density probe was correlated with CDW data determined in triplicate by sterile filtration. For this purpose  $5 \text{ mL}$  of fresh sample stored on ice was applied on a pre-weighed cellulose acetate filter ( $0.2 \mu\text{m}$ , Sartorius, Germany) vacuum filtrated and washed twice with  $5 \text{ mL}$  of chilled deionized water. Afterwards the filters were dried at  $105 \text{ }^\circ\text{C}$  for  $24 \text{ h}$ , cooled off in a desiccator and weighed again. The CDW ( $\text{g L}^{-1}$ ) was calculated with the following linear equation ( $R^2 = 0.9918$ ):  $\text{CDW} = 1.3132\text{OD} - 0.0149$  where OD is the centered moving average of the raw optical density probe signal over a  $21 \text{ min}$  period.

#### 2.5. Design of Experiments (DoE)

A total of four continuous fermentations (design 1 to 4) were carried out in this study. Each of them was based on an irregular fraction design (IFD), which consisted of several experiments with up to four different factors and three levels each. Only independent factors which were

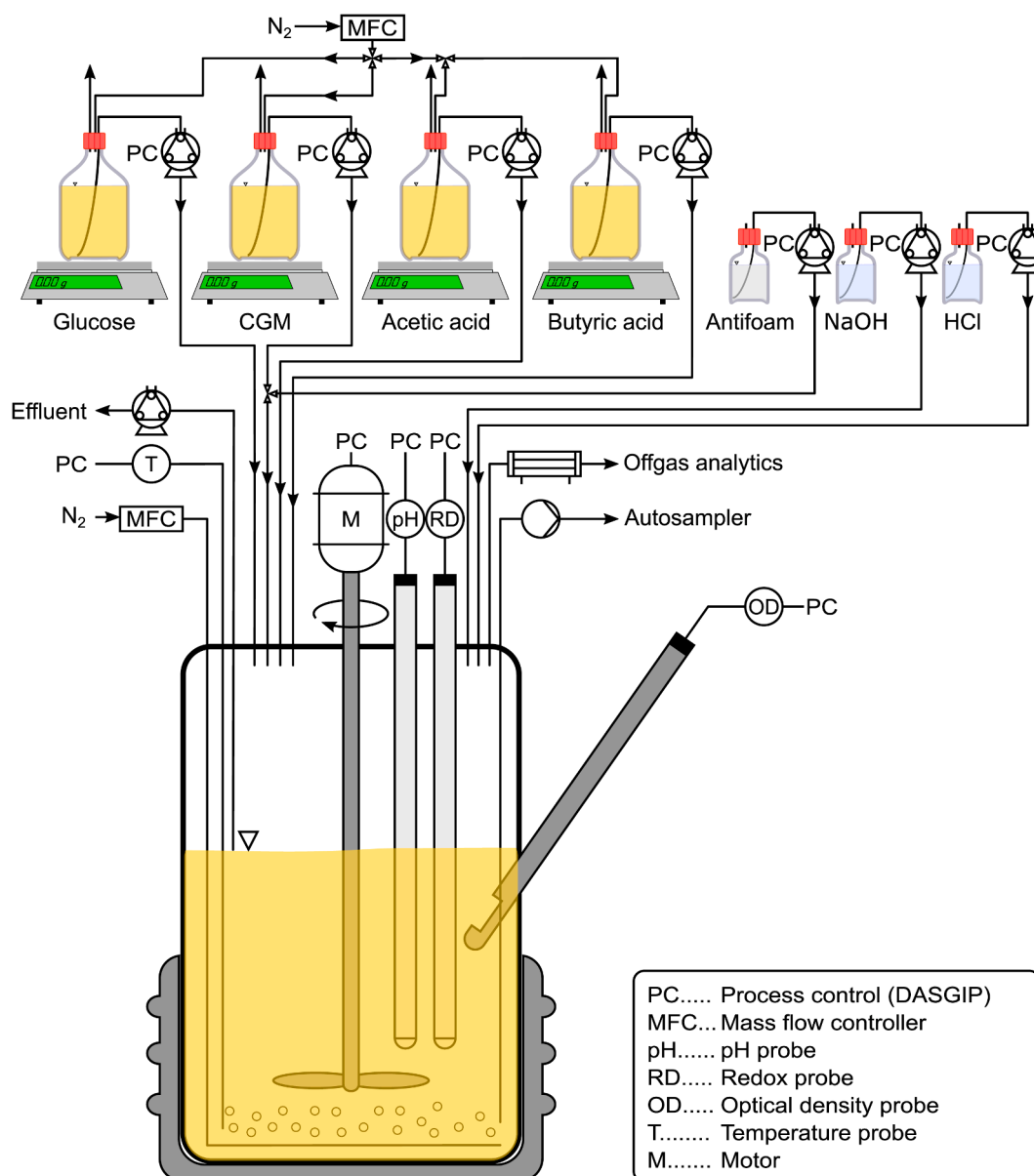


Fig. 1. Schematic of the reactor setup for the continuous fermentation experiments.

expected to have an impact on both, the specific uptake rate of butyric and acetic acid, were considered. The selection of factors and the determination of their initial boundaries were based on preliminary internal experiments that investigated the influence of butyric acid and acetic acid pulses at different pH on the specific butanol production rate (data not shown). All factors including their respective boundaries in the various designs and their evolution over time are provided in Table 1 and discussed in more detail in the following sections.

The experiments during the continuous fermentations were carried out as follows: after an initial batch phase of 12 h the feed pumps, effluent pumps and pH control were set to meet the experiment settings specified in the according IFD. Each experiment had to be operated for at least three residence times in order to be considered for statistical analysis. Additionally, a ‘criterion of stability’ had to be fulfilled before proceeding with the next experiment. This criterion was determined by the standard deviation of the CO<sub>2</sub> offgas over one quarter of a residence time via a sliding window operation and was met, if this deviation was below a threshold value of 0.25 (empirically determined based on preliminary experiments) during the last residence time. This was also the time frame over which each experiment was evaluated as can be seen in Section 2.6. To ensure that any possible time-dependent effects such as cultural degeneration did not bias the results, experiments with center point settings were conducted at the beginning, middle and end of each continuous fermentation. Since some settings led to a cell washout, affected experiments could not be operated for the intended time period and had to be aborted. As a consequence, the experimental design evolved between individual fermentations. The final IFD was an optimization of design 2. Based on the top 5 experiments regarding the highest specific production rate of butanol among the non-center experiments, a new design space was conceived. The additionally required experiments were performed in design 3. Design 4 consisted of three additional center points (having the same settings as in design 3) to increase model error accuracy, and two validation experiments. In Table 2 all experiments from design 2, 3 and 4, based on which the final models were calculated from, are listed. Before performing multiple linear regression (MLR) analysis the data was checked for potential collinearity between factors via pair plot, correlation coefficient and variance inflation factor (VIF). All of the statistical calculations were carried out using the python package statsmodels version 0.12.0 (Seabold and Perktold, 2010). The best models were chosen based on the akaike information criteria (AIC). This was done by removing insignificant (p-values above  $\alpha = 0.05$ ) factors from the models step by step with the goal of minimizing AIC. In the following sections, we describe the rationale for selecting and defining the boundaries of the DoE factors evaluated in this contribution.

### 2.5.1. pH

The influence of pH is known to be a key factor for solvent production, different reports of its optimum level range from 4.3 to 6.5 and are

**Table 1**  
DoE factors and their levels (low, center and high) per design (1 to 4).

factor	levels (low/center/high)		
	design 1	design 2	design 3 & 4
$F_c(acids)$	0.04	0.015	0.0097
	0.05	0.02	0.0183
	0.06	0.025	0.0270
$f_{acidratio}$	0	0	0
	0.5	0.5	0.5
	1	1	1
$f_{acids:glc}$	0.1	0.1	0.1
	0.6	0.3	0.26
	1.1	0.5	0.42
pH	4.8	4.8	fixed at 5.6
	5.5	5.2	
	6.2	5.6	

strain dependent (Jones and Woods, 1986). Preliminary DoE pulse experiments showed the highest butanol production rate to be at a pH of 4.8. At the same time this was the highest pH tested (other tested values were 4.2 and 4.5). Consequently, the optimum could lie at an even higher pH. Thus, 4.8 marked the lowest pH-level in this study. Several studies also using continuous cultures of *Clostridium saccharoperbutylacetonicum* report their pH is controlled at 5.5 (Oshiro et al., 2010; Tashiro et al., 2004; Gao et al., 2016; Baba et al., 2012). It was therefore considered to be an adequate center point. Eventually, the highest level for the factor pH was chosen to be 6.2 in order to maintain a symmetrical design space. During the course of the study the boundaries were first redefined to cover a more narrow pH range (design 2). High pH was considered less favorable as the culture should be kept in a predominantly solventogenic state. Additionally this could lead to high and undesired concentrations of salt ions due to increased rates of NaOH addition to control the pH. Since in design 2 the factor pH in the range between 4.8 to 5.6 had no significant effect on both, the specific butyric acid and specific acetic acid uptake rate, this factor was set to a fixed value of 5.6 in design 3. This was based on the experience with previous experiments, where a low pH often resulted in unstable fermentations. Between two experiments with different pH, it was slowly changed at a rate of 0.08 h<sup>-1</sup>.

### 2.5.2. Total feed rate of organic acids

Feed rates denoted as  $F_c$  are given in moles of carbon per liter and hour (mol L<sup>-1</sup> h<sup>-1</sup>). The total feed rate of organic acids fed during continuous fermentation can be expressed as  $F_c(acids) = F_c(aceac) + F_c(butac)$  where  $F_c(aceac)$  is the feed rate of acetic acid and  $F_c(butac)$  the feed rate of butyric acid. Since we studied the feed of organic acids (derived from the carboxylate platform)  $F_c(acids)$  can also be seen as a key factor to examine how the feed influences butanol production and acid uptake. Based on preliminary batch experiments where we fed acetic and butyric acid pulses to measure their respective uptake through the culture, we calculated, under the assumption that both acids get taken up simultaneously, a maximum acid uptake rate of -0.0434 mol L<sup>-1</sup> h<sup>-1</sup>. Since we were aiming at high uptake rates, this was our estimated baseline. This is a delicate estimate, considering that butyric acid has long been known to have a growth inhibitory effect on *Clostridium saccharoperbutylacetonicum* depending on its concentration and the presence of other substances such as butanol (Soni et al., 1987). In fact, design 1 revealed that our first estimate was inaccurate, as high butyric acid feed rates above 0.025 mol L<sup>-1</sup> h<sup>-1</sup> (at centerpoint settings) resulted in excessive concentrations that consequently led to unstable fermentations. Therefore, this value was set as the new high level in design 2. As already mentioned in Section 2.5 the design space for design 3 and 4 was further optimized based on experiments from design 2 which showed the highest specific production rates of butanol.

### 2.5.3. Normalized factor of the feed rate ratio between acetic and butyric acid

The normalized factor of the feed rate ratio between acetic and butyric acid is defined as  $f_{acidratio} = F_c(aceac)/F_c(acids) = 1 - F_c(butac)/F_c(acids)$ . Consequently, if  $f = 0 \Rightarrow F_c(acids) = F_c(butac)$  and if  $f = 1 \Rightarrow F_c(acids) = F_c(aceac)$ . To study both, separate and combined effects, the levels were chosen so that the carboxylic acid feed rate either consisted of acetic acid only, butyric acid only, or a mixture of both.

### 2.5.4. Ratio between total acid feed rate and glucose feed rate

The ratio between total acid feed rate and glucose feed rate is defined as  $f_{acids:glc} = F_c(acids)/F_c(glc)$  where  $F_c(glc)$  is the feed rate of glucose. Since glucose is needed for cell growth, as well as for the conversion of organic acids to solvents, we coupled the glucose feed rate to the acid feed rate. This should lead us to settings where excess glucose in the effluent can be prevented. As a guideline for the high level boundary we took the reported maximal ratio of 1.6 mol mol<sup>-1</sup> butyric acid/glucose

**Table 2**

Final design space of IFD including design number, experiment type, target and actual factor settings.

#	design	type <sup>a</sup>	$F_c(acids)$		$f_{acidratio}$		$f_{acids:glc}$	
			target	actual	target	actual	target	actual
1	3	tds, cp	0.0183	0.0190	0.5	0.5367	0.2611	0.2727
2	3	tds	0.0270	0.0300	1	1	0.4215	0.4702
3	2	tds	0.0150	0.0114	0	0	0.1000	0.0748
4	3	tds	0.0097	0.0109	1	1	0.4215	0.5557
5	2	tds	0.0150	0.0136	0	0	0.5000	0.2529
6	3	tds	0.0270	0.0258	0	0	0.4215	0.4018
7	3	tds, cp	0.0183	0.0193	0.5	0.5425	0.2611	0.2750
8	3	unstable	0.0270	0.0314	1	1	0.1007	0.1182
9	2	tds	0.0150	0.0097	1	1	0.1000	0.0642
10	2	outlier	0.0250	0.0270	0	0	0.1000	0.1050
11	3	tds	0.0270	0.0263	0	0	0.1750	0.1681
12	3	tds, cp	0.0183	0.0194	0.5	0.5358	0.2611	0.2796
13	2	tds	0.0250	0.0162	1	1	0.1000	0.0604
14	4	tds, cp	0.0183	0.0194	0.5	0.5322	0.2611	0.2782
15	4	val	0.0230	0.0230	0.2	0.2161	0.4000	0.4046
16	4	tds, cp	0.0183	0.0195	0.5	0.5381	0.2611	0.2824
17	4	val	0.0230	0.0232	0.2	0.2139	0.4000	0.3955
18	4	tds, cp	0.0183	0.0194	0.5	0.5389	0.2611	0.2765

<sup>a</sup>tds: training data set, included in model; cp: center point; unstable: not included in models; outlier: not included in models; val: validation experiment, not included in models

obtained in fed-batch fermentations with *Clostridium saccharoperbutylacetonicum* by Tashiro et al. (2004), which calculates to a ratio of 1.067 when based on moles of carbon. In contrast, Richter et al. (2012) reported the ratio to be 0.239 (based on moles of carbon) in continuous culture. Own preliminary batch experiments have shown that the concentration ratio of organic acids to glucose in the fermenter lies between 0.34 to 0.47. No experiment in design 1 showed any glucose limitation; instead, glucose would often rise to high concentrations (up to 98 g L<sup>-1</sup>) in the fermenter. This is undesirable for two reasons: First, from an economic standpoint caused by the loss of valuable substrate through the effluent. Second, high glucose concentrations can cause product and/or substrate inhibition. This is typically a problem with batch fermentations where glucose concentrations of 60 g L<sup>-1</sup> and 162 g L<sup>-1</sup> lead to product and substrate inhibition, respectively (Ezeji et al., 2004). To avoid these problems in the future, the range was reduced in design 2, but the settings of the center point in terms of glucose feed rate remained the same as in design 1. Level settings in design 3 and 4 for  $f_{acids:glc}$  had been optimized slightly based on the results from the experiments of design 2.

### 2.6. Calculations

The uptake or production rate ( $r$ / g h<sup>-1</sup>) for a substrate or product, respectively, was calculated according to Eq. 1:

$$r = (-1) \left( c_{in} F_{in} - c_{out} D V_r - \frac{V_r (c_{out,t_1} - c_{out,t_0})}{t_1 - t_0} \right) \quad (1)$$

where  $c_{in}$  is the concentration of the substrate or product in the feed (g L<sup>-1</sup>),  $F_{in}$  the flow rate of the feed (L h<sup>-1</sup>),  $c_{out}$  the concentration of the substrate or product in the effluent (g L<sup>-1</sup>; the additional subscript  $t$  denotes at which sampling time),  $D$  the overall dilution rate (h<sup>-1</sup>),  $V_r$  the reactor volume (L), and  $t$  the sampling time (h). It applies that  $c_{out} = c_{out,t}$ . By convention, negative rates represent the uptake and positive values represent the production of substances. Specific rates ( $q$ / g g<sup>-1</sup> h<sup>-1</sup>) were calculated by Eq. 2:

$$q = \frac{r}{\frac{x_0 + x_t}{2} V_r} \quad (2)$$

where  $x_t$  is the CDW (g L<sup>-1</sup>) at sampling time  $t$  (h).

### 3. Results and discussion

Exemplary for all experiments a center point experiment (#7 in Table 2) in Fig. 2 shows the time course of substrate, product, cell and offgas concentrations together with the computed specific rates as described in Section 2.6. The mean values of the specific rates during the last residence time (as marked in Fig. 2) of each experiment were used as responses for statistical analysis. Visible periodic fluctuations in the offgas were caused by the addition of antifoam. Before building the linear regression models, the data was checked for possible outliers. In this process, the suspicious lone 'top performer' in terms of the highest specific butanol production rate ( $q_{butOH}$ ) from design 2 was removed from the dataset, as the result could not be confirmed in design 3. The last experiment of design 3 was removed as well, since it did not meet the 'criterion of stability' defined in Section 2.5. Since the data showed no evidence of collinearity, linear regression models were calculated starting with all factors as described in Section 2.5 under the consideration of possible factor interactions. The best (based on the AIC) obtained model for the specific uptake rate of butyric acid ( $q_{butac}$ ) can be described by the model term in Eq. 3:

$$q_{butac} = 0.0207 - 9.4561 F_c(acids) + 0.0303 f_{acidratio} + 8.0285 F_c(acids) f_{acidratio} \quad (3)$$

Fig. 3A shows the ability of the model to predict the actual data. The two validation experiments, which were not part of the training dataset for the linear regression, also confirm the high prediction capability of the model. Error bars in Fig. 3B not exceeding  $y = 0$  demonstrate that the total organic acid feed rate ( $F_c(acids)$ ), the normalized factor of the feed rate ratio between acetic and butyric acid ( $f_{acidratio}$ ) as well as their interaction with each other, are statistically significant ( $\alpha = 0.05$ ) factors of the model for  $q_{butac}$ . Having the largest distance to  $y = 0$ ,  $f_{acidratio}$  has the highest relative impact in this model. The response of the model for  $q_{butac}$  depending on the factor settings of  $F_c(acids)$  and  $f_{acidratio}$  is shown in Fig. 3C. It can be seen that in the case where almost no butyric acid has been fed ( $f_{acidratio} \rightarrow 1$ ) and  $F_c(acids)$  is low, butyric acid is produced instead of taken up. This likely comes from the fact that the fermentation is not purely in a solventogenic state meaning that the growing, acetogenic cells still produce acids.

For the specific uptake rate of acetic acid ( $q_{aceac}$ ) the best obtained model can be described by Eq. 4:

$$q_{aceac} = 0.0334 + 1.5013 F_c(acids) + 0.0432 f_{acidratio} - 16.5844 F_c(acids) f_{acidratio} \quad (4)$$

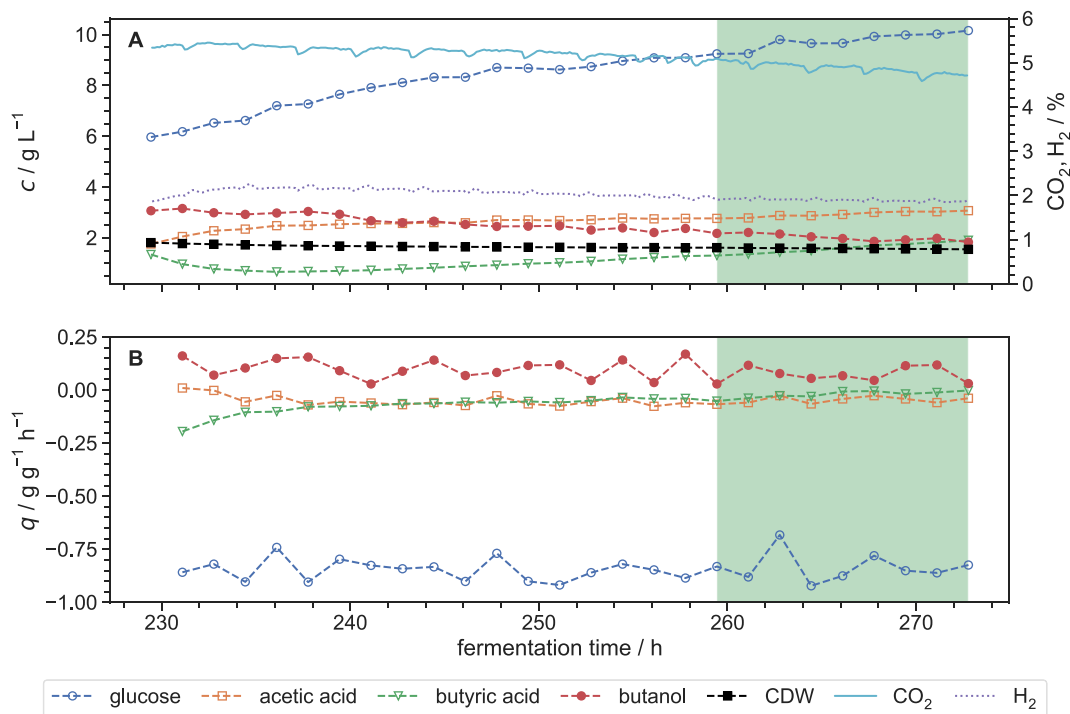


Fig. 2. Evolution of substrate, product, cell, CO<sub>2</sub> and H<sub>2</sub> concentrations (A) as well as the computed specific rates (B) during center point experiment 7 in design 3. The highlighted section marks the last residence time in this experiment.

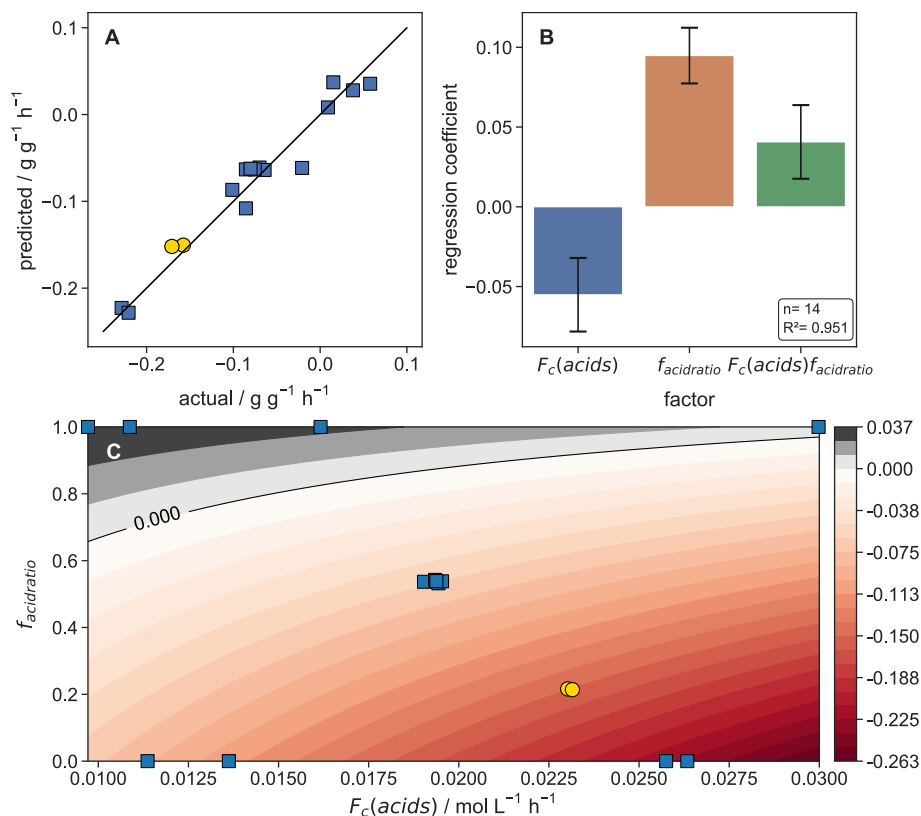


Fig. 3. Model plots for the specific butyric acid uptake rate ( $q_{buac}$ ). Square symbols indicate model training data and circle symbols indicate validation experiments. A: Model prediction versus actual observed  $q_{buac}$ . B: Regression coefficients with coded/normalized factors (-1 to 1). Relative impact of model terms increases with distance to  $y = 0$ . Error bars represent the 95 % confidence interval. C: Model prediction of  $q_{buac}$  based on factor settings of  $F_c(acids)$  and  $f_{acidratio}$ .

Its ability to predict the actual data is shown in Fig. 4A. Likewise, the validation experiments confirm the high prediction capability of the model. However, it should be noted that the bottom left point of the training dataset in Fig. 4A has a big leverage on the model, but excluding it does change the model only negligibly. As nothing indicates an outlier, it has been left in the model. The coefficients as shown in Fig. 4B reveal a similar picture than that of the model for  $q_{butac}$ . Again  $F_c(acids)$ ,  $f_{acidratio}$  and their interaction with each other, are statistically significant ( $\alpha = 0.05$ ) factors of the model and once more,  $f_{acidratio}$  has the highest relative impact. Fig. 4C shows the response of the model for  $q_{aceac}$  depending on the factor settings of  $F_c(acids)$  and  $f_{acidratio}$ . Analogously to the model for  $q_{butac}$ , it can be seen that at low levels of  $F_c(acids)$  and the more  $f_{acidratio} \rightarrow 0$ , there is a region in which acetic acid is produced rather than taken up.

The ratio between total acid feed rate and glucose feed rate ( $f_{acids:glc}$ ) was not a significant factor in either of our models. This suggests that maintaining a low level of glucose in the broth is sufficient, thereby preventing its loss through the effluent. Another finding was that the upper limit for  $F_c(acids)$ , where a still stable continuous fermentation process could be operated, was at  $0.030 \text{ mol L}^{-1} \text{ h}^{-1}$ . Since both attempts to operate the fermentation with factors set like experiment 8 (see Table 2) resulted in a wash out of cells (initial attempt only running for 28.33 h, second attempt running for 46.28 h with an actual  $F_c(acids)$  of  $0.0305 \text{ mol L}^{-1} \text{ h}^{-1}$  and  $0.0314 \text{ mol L}^{-1} \text{ h}^{-1}$ , respectively) this is likely very close to the true limit. Hence, in order to minimize excess glucose in the effluent and maximize the butyric acid uptake rate, we propose the following optimal factor settings:  $F_c(acids) = 0.03 \text{ mol L}^{-1} \text{ h}^{-1}$ ,  $f_{acidratio} = 0$  and  $f_{acids:glc} = 0.56$ . If instead  $q_{aceac}$  is to be maximized, acetic acid must be the only carboxylic acid in the feed ( $f_{acidratio} = 1$ ). Aiming for the latter, however, has no significant impact on the specific production rate of butanol ( $q_{butOH}$ ). Only the specific uptake rates of both butyric acid ( $q_{butac}$ ) and glucose ( $q_{glc}$ ) do have significant effects, as

indicated by the following model equation Eq. 5:

$$q_{butOH} = 0.0192 - 0.0697q_{glc} + 0.2815q_{butac} - 0.6266q_{glc}q_{butac} \quad (5)$$

Fig. 5B depicts all significant factors and their relative impact on the model for  $q_{butOH}$ . Although  $q_{glc}$  has the biggest influence,  $q_{butac}$  plays an important role in the production of butanol as well. The response of the model for  $q_{butOH}$  depending on both of those factors is shown in Fig. 5C. At this point it should be noted that within an experiment, the standard deviation of  $q_{butOH}$  can range from 0.022 to 0.083, leading to more uncertainty in the model than in the models for  $q_{butac}$  and  $q_{aceac}$ . This becomes evident after considering its prediction capability in Fig. 5A. The increased uncertainty is a direct cause of the measured concentrations of butanol, which tend to vary more over time than that of other measured substances like glucose or carboxylic acids. The reason, in turn, could be a varying loss of the more volatile butanol due to an unintentional gas stripping effect originating from changing offgas flow rates and other factors such as antifoam additions, despite precautions like offgas cooling.

It has been reported previously that the co-feeding of acetate with glucose during a pH-stat batch fermentation does improve butanol and acetone production (Gao et al., 2016). Another study concerning fed-batch cultures instead found no impact on feeding of acetic acid on enhancing butanol production (Tashiro et al., 2004). The presented statistical model for  $q_{butOH}$  extends the knowledge in this area for continuous fermentations, by demonstrating how butanol production is influenced by  $q_{glc}$  and  $q_{butac}$ , creating a true physiological based process understanding. Additionally, Fig. 3,4 give a clear picture of how controllable factors affect the response of the culture and within which boundaries a stable continuous process can be operated. The factors and responses used to calculate all the models presented are shown in Table 3.

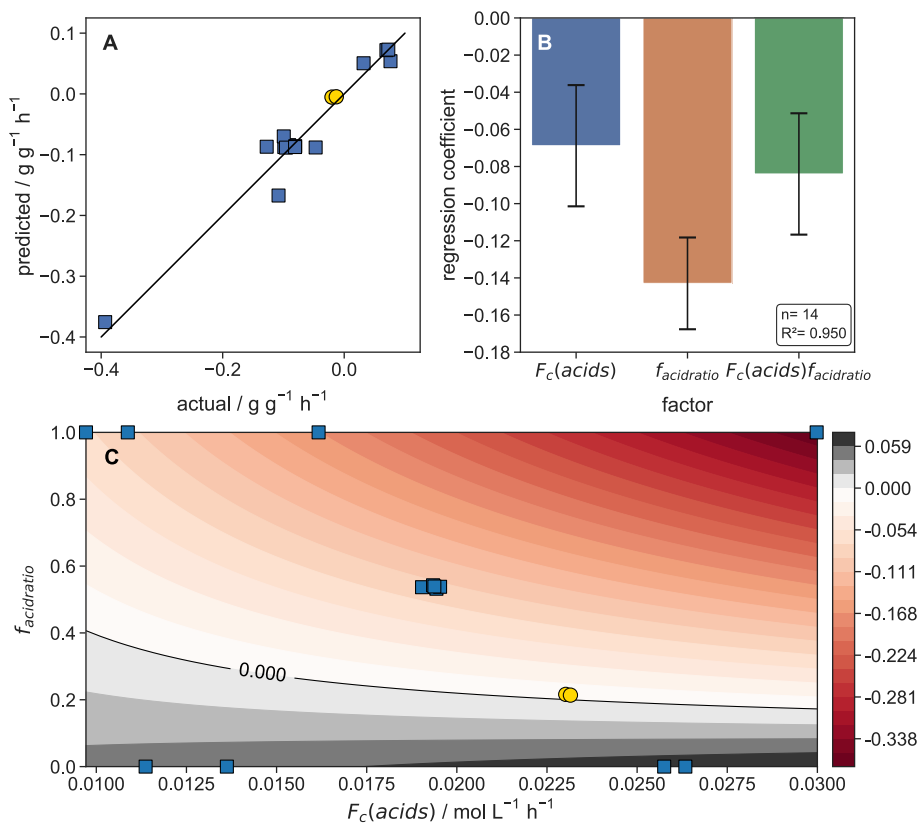
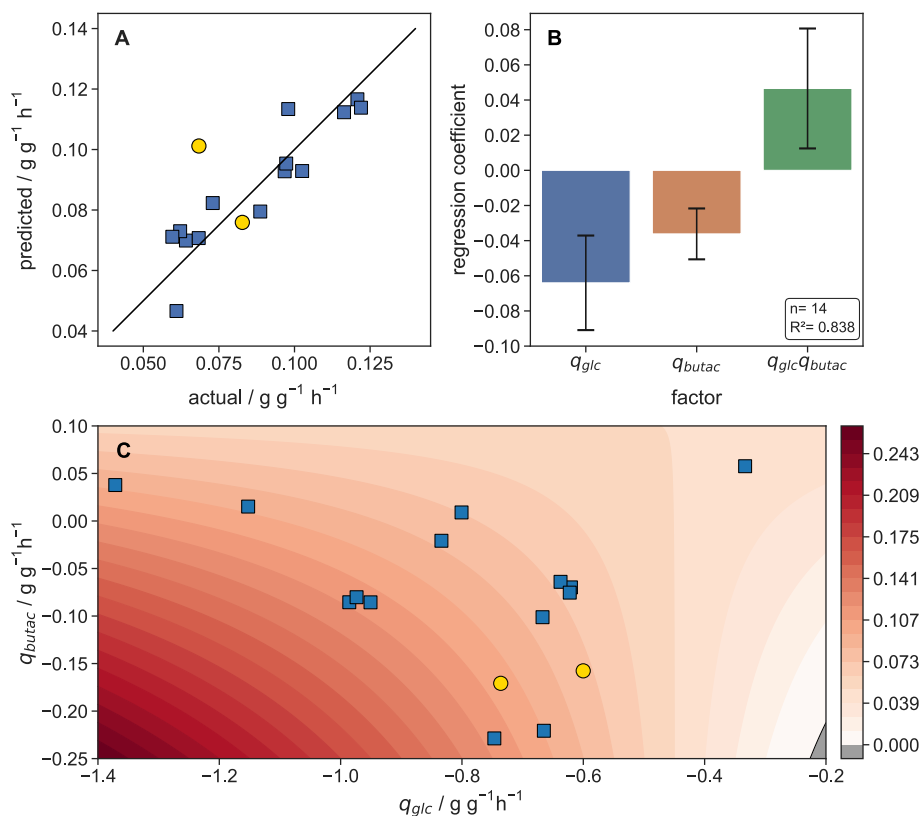


Fig. 4. Model plots for the specific acetic acid uptake rate ( $q_{aceac}$ ). Square symbols indicate model training data and circle symbols indicate validation experiments. A: Model prediction versus actual observed  $q_{aceac}$ . B: Regression coefficients with coded/normalized factors (-1 to 1). Relative impact of model terms increases with distance to  $y = 0$ . Error bars represent the 95 % confidence interval. C: Model prediction of  $q_{aceac}$  based on factor settings of  $F_c(acids)$  and  $f_{acidratio}$ .



**Fig. 5.** Model plots for the specific butanol production rate ( $q_{butOH}$ ). Square symbols indicate model training data and circle symbols indicate validation experiments. A: Model prediction versus actual observed  $q_{butOH}$ . B: Regression coefficients with coded/normalized factors (-1 to 1). Relative impact of model terms increases with distance to  $y = 0$ . Error bars represent the 95 % confidence interval. C: Model prediction of  $q_{butOH}$  based on factor settings of  $q_{glc}$  and  $q_{butac}$ .

The performance of several different experiments during prolonged continuous fermentations presented two main challenges: First, not every setpoint had a stable point of operation, which consequently meant that the design space had to be adapted multiple times. The second challenge was the long operating times, which required an automatic, high-frequency sampling strategy and the ability to continuously measure the biomass concentration in order to reliably calculate the rates. No time-dependent effect could be detected upon examining

the evenly spread center point experiments, so the condition of time independence was satisfied. Furthermore, conducting the validation experiments together with additional center point experiments in an individual, separate design, confirmed that a comparability between the different designs is given.

As reviewed by [Mayank et al. \(2013\)](#), the development of mathematical models related to ABE fermentation is not new. The downside of stoichiometric models with their inability to reflect real time dynamics

**Table 3**

Factors and responses of final IFD used for the models (with the exception of #15 and #17, which were used for validation only). Moles in units must be considered as moles of carbon.

#	$F_c$ (acids) (mol L <sup>-1</sup> h <sup>-1</sup> )	$f_{acidratio}$	$f_{acids:glc}$ (mol mol <sup>-1</sup> )	$q_{butac}$ (g g <sup>-1</sup> h <sup>-1</sup> )	$q_{aceac}$ (g g <sup>-1</sup> h <sup>-1</sup> )	$q_{butOH}$ (g g <sup>-1</sup> h <sup>-1</sup> )	$q_{glc}$ (g g <sup>-1</sup> h <sup>-1</sup> )
1	0.0190	0.5367	0.2727	-0.0698	-0.0907	0.0641	-0.6204
2	0.0300	1	0.4702	0.0090	-0.3934	0.0622	-0.8007
3	0.0114	0	0.0748	-0.1012	0.0319	0.0887	-0.6672
4	0.0109	1	0.5557	0.0576	-0.0986	0.0610	-0.3333
5	0.0136	0	0.2529	-0.0855	0.0762	0.1208	-0.9858
6	0.0258	0	0.4018	-0.2287	0.0695	0.1220	-0.7467
7	0.0193	0.5425	0.2750	-0.0208	-0.0470	0.0730	-0.8339
8	0.0314	1	0.1182	0.0796	-0.1917	0.0075	-0.6789
9	0.0097	1	0.0642	0.0152	-0.0995	0.0967	-1.1524
10	0.0270	0	0.1050	-0.4291	0.1590	0.1611	-1.3810
11	0.0263	0	0.1681	-0.2207	0.0726	0.0973	-0.6650
12	0.0194	0.5358	0.2796	-0.0856	-0.1276	0.1164	-0.9508
13	0.0162	1	0.0604	0.0378	-0.1081	0.1025	-1.3715
14	0.0194	0.5322	0.2782	-0.0640	-0.0806	0.0596	-0.6375
15	0.0230	0.2161	0.4046	-0.1577	-0.0201	0.0828	-0.6001
16	0.0195	0.5381	0.2824	-0.0754	-0.0959	0.0683	-0.6223
17	0.0232	0.2139	0.3955	-0.1708	-0.0131	0.0684	-0.7361
18	0.0194	0.5389	0.2765	-0.0802	-0.0809	0.0979	-0.9737



has been overcome by kinetic models such as that of Shinto et al. (2007); Shinto et al., 2008 which were later refined by Li et al. (2011). However, they were based on batch fermentations as well as the utilization of either glucose or xylose. A more recent work of Dfáz and Willis (2018) also took into account carbon catabolite repression using historic data of continuous fermentations. In comparison to this work, we took a different approach by using DoE and additionally focusing on carboxylic acid uptake instead of monomeric sugars. Furthermore, the ability to shape the design space in which we conducted our experiments allowed us to gain insights on a physiological level. In addition, process limitations were revealed and optimal feeding strategies were identified.

Summarized, it can be concluded that in order to maximize the specific butanol production rate, glucose uptake rate is an influential factor but at the same time the concentration in the broth can be controlled at low levels to only support the current demand. Based on our data, we suggest that fermentation should ideally be controlled at a specific glucose feed rate of around  $0.75 \text{ g g}^{-1} \text{ h}^{-1}$ . Of course, this must be further optimized depending on the specific setup. Since we found that acetic acid has no positive effect on butanol production, any upstream carboxylate process should be shifted towards butyric rather than acetic acid. In addition, the butyric acid feed rate should be controlled in a way that a maximum uptake rate is achieved without causing detrimental concentration effects which ultimately lead to unstable fermentations. According to our model in Eq. 3, this would result in a specific butyric acid feed rate of  $0.26 \text{ g g}^{-1} \text{ h}^{-1}$ .

#### 4. Conclusions

This work contributes to an efficient production of butanol with respect to a multi-feedstock biorefinery by providing mathematical relationships between substrate-dependent factors and physiological response factors as well as showing the limits within which a stable continuous fermentation process can be maintained. Key success factor was the novel combination of sophisticated bioprocessing with a high frequency monitoring strategy to implement an evolving DoE. The discovered physiologically scalable dependence of  $q_{butac}$  and  $q_{glc}$  on  $q_{butOH}$  can be applied for controlling bioprocesses with complex carboxylate-based substrates and transferred to other bioreactor designs, for example one with continuous butanol removal and/or cell retention.

#### CRedit authorship contribution statement

**Florian Gattermayr:** Conceptualization, Methodology, Validation, Formal analysis, Investigation, Writing - original draft, Writing - review & editing, Visualization. **Christoph Herwig:** Supervision, Writing - review & editing. **Viktoria Leitner:** Conceptualization, Project administration, Writing - review & editing.

#### Declaration of Competing Interest

The authors declare that they have no known competing financial interests or personal relationships that could have appeared to influence the work reported in this paper.

#### Acknowledgement

This work was supported by the European Regional Development Fund (EFRE) and the province of Upper Austria.

#### References

Aglar, M.T., Wrenn, B.A., Zinder, S.H., Angenent, L.T., 2011. Waste to bioproduct conversion with undefined mixed cultures: the carboxylate platform. *Trends Biotechnol.* 29, 70–78. <https://doi.org/10.1016/j.tibtech.2010.11.006>.  
 Arslan, D., 2014. Selective Short Chain Carboxylates Production by Mixed Culture Fermentation. Ph.D. thesis. Wageningen University. Wageningen.

Baba, S.i., Tashiro, Y., Shinto, H., Sonomoto, K., 2012. Development of high-speed and highly efficient butanol production systems from butyric acid with high density of living cells of *Clostridium saccharoperbutylacetonicum*. *Journal of Biotechnology* 157, 605–612. doi: 10.1016/j.jbiotec.2011.06.004.  
 Bahl, H., Andersch, W., Braun, K., Gottschalk, G., 1982. Effect of pH and butyrate concentration on the production of acetone and butanol by *Clostridium acetobutylicum* grown in continuous culture. *Eur. J. Appl. Microbiol. Biotechnol.* 14, 17–20. <https://doi.org/10.1007/BF00507998>.  
 Chen, C.K., Blaschek, H.P., 1999. Acetate enhances solvent production and prevents degeneration in *Clostridium beijerinckii* BA101. *Appl. Microbiol. Biotechnol.* 52, 170–173. <https://doi.org/10.1007/s002530051504>.  
 Cherubini, F., Jungmeier, G., Wellisch, M., Willke, T., Skiadas, I., Van Ree, R., de Jong, E., 2009. Toward a common classification approach for biorefinery systems. *Biofuels, Bioprod. Biorefin.* 3, 534–546. <https://doi.org/10.1002/bbb.172>.  
 Dfáz, V.H.G., Willis, M.J., 2018. Kinetic modelling and simulation of batch, continuous and cell-recycling fermentations for acetone-butanol-ethanol production using *Clostridium saccharoperbutylacetonicum* N1–4. *Biochem. Eng. J.* 30–39 <https://doi.org/10.1016/j.bej.2018.05.011>.  
 Elbeshbishy, E., Dhar, B.R., Hafez, H., Lee, H.S., 2015. Acetone-butanol-ethanol production in a novel continuous flow system. *Bioresour. Technol.* 190, 315–320. <https://doi.org/10.1016/j.biortech.2015.04.081>.  
 Ezeji, T.C., Qureshi, N., Blaschek, H.P., 2004. Acetone butanol ethanol (ABE) production from concentrated substrate: reduction in substrate inhibition by fed-batch technique and product inhibition by gas stripping. *Appl. Microbiol. Biotechnol.* 63, 653–658. <https://doi.org/10.1007/s00253-003-1400-x>.  
 Fond, O., Matta-Ammouri, G., Petitdemange, H., Engasser, J.M., 1985. The role of acids on the production of acetone and butanol by *Clostridium acetobutylicum*. *Appl. Microbiol. Biotechnol.* 22, 195–200. <https://doi.org/10.1007/BF00253609>.  
 Gao, M., Tashiro, Y., Wang, Q., Sakai, K., Sonomoto, K., 2016. High acetone-butanol-ethanol production in pH-stat co-feeding of acetate and glucose. *J. Biosci. Bioeng.* 122, 176–182. <https://doi.org/10.1016/j.jbiosc.2016.01.013>.  
 Grupe, H., Gottschalk, G., 1992. Physiological Events in *Clostridium acetobutylicum* during the Shift from Acidogenesis to Solventogenesis in Continuous Culture and Presentation of a Model for Shift Induction. *Appl. Environ. Microbiol.* 58, 3896–3902. <https://doi.org/10.1128/AEM.58.12.3896-3902.1992>.  
 Herrero, A.A., 1983. End-product inhibition in anaerobic fermentations. *Trends Biotechnol.* 1, 49–53. [https://doi.org/10.1016/0167-7799\(83\)90069-0](https://doi.org/10.1016/0167-7799(83)90069-0).  
 Holtzapfel, M.T., Granda, C.B., 2009. Carboxylate Platform: The MixAlco Process Part 1: Comparison of Three Biomass Conversion Platforms. *Appl. Biochem. Biotechnol.* 156, 95–106. <https://doi.org/10.1007/s12010-008-8466-y>.  
 Hüsemann, M.H.W., Papoutsakis, E.T., 1988. Solventogenesis in *Clostridium acetobutylicum* fermentations related to carboxylic acid and proton concentrations. *Biotechnology and Bioengineering* 32, 843–852. doi: 10.1002/bit.260320702.  
 Jones, D.T., Woods, D.R., 1986. Acetone-butanol fermentation revisited. *Microbiol. Rev.* 50, 484–524.  
 Li, R.D., Li, Y.Y., Lu, L.Y., Ren, C., Li, Y.X., Liu, L., 2011. An improved kinetic model for the acetone-butanol-ethanol pathway of *Clostridium acetobutylicum* and model-based perturbation analysis. *BMC Syst. Biol.* 5, S12. <https://doi.org/10.1186/1752-0509-5-S1-S12>.  
 Maddox, I.S., Steiner, E., Hirsch, S., Wessner, S., Gutierrez, N.A., Gapes, J.R., Schuster, K.C., 2000. The Cause of Acid Crash and Acidogenic Fermentations During the Batch Acetone-Butanol-Ethanol (ABE-) Fermentation Process. *J. Mol. Microbiol. Biotechnol.* 2, 95–100.  
 Matta-El-Ammouri, G., Janati-Idrissi, R., Junelles, A.M., Petitdemange, H., Gay, R., 1987. Effects of butyric and acetic acids on acetone-butanol formation by *Clostridium acetobutylicum*. *Biochimie* 69, 109–115. [https://doi.org/10.1016/0300-9084\(87\)90242-2](https://doi.org/10.1016/0300-9084(87)90242-2).  
 Mayank, R., Ranjan, A., Moholkar, V.S., 2013. Mathematical models of ABE fermentation: review and analysis. *Crit. Rev. Biotechnol.* 33, 419–447. <https://doi.org/10.3109/07388551.2012.726208>.  
 Monot, F., Martin, J.R., Petitdemange, H., Gay, R., 1982. Acetone and Butanol Production by *Clostridium acetobutylicum* in a Synthetic Medium. *Appl. Environ. Microbiol.* 44, 1318–1324. <https://doi.org/10.1128/aem.44.6.1318-1324.1982>.  
 Mutschlechner, O., Swoboda, H., Gapes, J.R., et al., 2000. Continuous two-stage ABE-fermentation using *Clostridium beijerinckii* NRRL B 592 operating with a growth rate in the first stage vessel close to its maximal value. *J. Mol. Microbiol. Biotechnol.* 2, 101–105.  
 Oshiro, M., Hanada, K., Tashiro, Y., Sonomoto, K., 2010. Efficient conversion of lactic acid to butanol with pH-stat continuous lactic acid and glucose feeding method by *Clostridium saccharoperbutylacetonicum*. *Appl. Microbiol. Biotechnol.* 87, 1177–1185. <https://doi.org/10.1007/s00253-010-2673-5>.  
 Richter, H., Qureshi, N., Heger, S., Dien, B., Cotta, M.A., Angenent, L.T., 2012. Prolonged conversion of n-butyrate to n-butanol with *Clostridium saccharoperbutylacetonicum* in a two-stage continuous culture with in-situ product removal. *Biotechnol. Bioeng.* 109, 913–921. <https://doi.org/10.1002/bit.24380>.  
 Seabold, S., Perktold, J., 2010. statsmodels: Econometric and statistical modeling with python. In: 9th python in science conference.  
 Shinto, H., Tashiro, Y., Kobayashi, G., Sekiguchi, T., Hanai, T., Kuriya, Y., Okamoto, M., Sonomoto, K., 2008. Kinetic study of substrate dependency for higher butanol production in acetone-butanol-ethanol fermentation. *Process Biochem.* 43, 1452–1461. <https://doi.org/10.1016/j.procbio.2008.06.003>.  
 Shinto, H., Tashiro, Y., Yamashita, M., Kobayashi, G., Sekiguchi, T., Hanai, T., Kuriya, Y., Okamoto, M., Sonomoto, K., 2007. Kinetic modeling and sensitivity analysis of acetone-butanol-ethanol production. *J. Biotechnol.* 12 <https://doi.org/10.1016/j.jbiotec.2007.05.005>.

- Soni, B.K., Das, K., Ghose, T.K., 1987. Inhibitory factors involved in acetone-butanol fermentation by *Clostridium saccharoperbutylacetonicum*. *Curr. Microbiol.* 16, 61–67. <https://doi.org/10.1007/BF01588173>.
- Standfest, T., 2013. Optimierung und alternative Substrate in der ABE-Fermentation mit *Clostridium acetobutylicum*. Ph.D. thesis. Universität Ulm.
- Tashiro, Y., Shinto, H., Hayashi, M., Baba, S.I., Kobayashi, G., Sonomoto, K., 2007. Novel high-efficient butanol production from butyrate by non-growing *Clostridium saccharoperbutylacetonicum* N1-4 (ATCC 13564) with methyl viologen. *Journal of Bioscience and Bioengineering* 104, 238–240. doi: 10.1263/jbb.104.238.
- Tashiro, Y., Takeda, K., Kobayashi, G., Sonomoto, K., Ishizaki, A., Yoshino, S., 2004. High butanol production by *Clostridium saccharoperbutylacetonicum* N1-4 in fed-batch culture with pH-Stat continuous butyric acid and glucose feeding method. *J. Biosci. Bioeng.* 98, 263–268. [https://doi.org/10.1016/S1389-1723\(04\)00279-8](https://doi.org/10.1016/S1389-1723(04)00279-8).
- Wiesenborn, D.P., Rudolph, F.B., Papoutsakis, E.T., 1988. Thiolase from *Clostridium acetobutylicum* ATCC 824 and Its Role in the Synthesis of Acids and Solvents. *Appl. Environ. Microbiol.* 54, 2717–2722. <https://doi.org/10.1128/aem.54.11.2717-2722.1988>.
- Zheng, J., Tashiro, Y., Yoshida, T., Gao, M., Wang, Q., Sonomoto, K., 2013. Continuous butanol fermentation from xylose with high cell density by cell recycling system. *Bioresour. Technol.* 129, 360–365. <https://doi.org/10.1016/j.biortech.2012.11.066>.